

Stability and quench development study in small HTSC magnet

Yu. A. Ilyin^{a,*}, V.S. Vysotsky^b, T. Kiss^c, M. Takeo^c, H. Okamoto^d, F. Irie^e

^a Low Temperature Division, Faculty of Applied Physics, University of Twente, P.O. Box 217, 7500AE Enschede, Netherlands

^b Institute of Superconductivity and Solid State Physics, RRC “Kurchatov Institute”, 123182 Moscow, Russia

^c Kyushu University, Graduate School of ISEE, Fukuoka 812-8581, Japan

^d Kyushu Electric Power Co., Fukuoka, Japan

^e Kyushu University, Fukuoka, Japan

Received 21 May 2001; accepted 10 September 2001

Abstract

Stability and quench development in a HTSC magnet have been experimentally studied with the transport current in the magnet being below or above the “thermal quench current” level. The magnet was tested at both cryocooler cooling and liquid nitrogen cooling, with and without background magnetic field (up to 4 T). The temperature and electrical voltages in different sections of the magnet were measured using 20 thermocouples and 24 potential taps embedded in the winding. In this paper, the experimental procedure and the results are described. The results are compared with those obtained earlier in the experiments with the smaller HTSC specimens and are analysed by using the scaling theory of the thermal quench. © 2001 Elsevier Science Ltd. All rights reserved.

Keywords: HTSC magnets; Stability; Quench

1. Introduction

Despite rather high stability of the HTSC Bi-based magnets with respect to heat disturbances, the thermal quench (TQ) may occur in them under certain circumstances [1–6]. That happens because of the strong non-linearity of the voltage–current characteristics in HT superconductors. If transport current in a HTSC coil exceeds certain magnitude – thermal quench current (TQC), then the internal heating power release becomes not balanced with the cooling and fast rise of the temperature and electrical voltages inside the coil is unavoidable, leading to the damage of the coil.

Starting with the short samples in our previous works [1–4], we continue to investigate the TQ with larger specimens. Recently the results and analysis of the experiments with the small pancake coil were reported [5]. We also developed a zero-dimensional theoretical scaling model [6] to describe the temperature and voltage behaviour in HTSC coils during quench, and extensively verified this model by many experimental data [5,6]. The

model permits to estimate the TQC, temperature, and voltage dependencies on time and characteristic times of a quench of HTSC coils.

To extend the study with larger specimens, the heavily instrumented HTSC magnet staked from two double pancake coils (four pancakes in total) has been tested. The magnet was fabricated by Sumitomo Electric Industries. The behaviour of the temperature and electrical voltages inside the magnet was studied under different initial temperatures (20–80 K), different values of external magnetic fields (0–4 T) and different cooling conditions. Cooling conditions included liquid nitrogen (LN₂) cooling and cryocooler cooling.

In this paper, the experimental results of the stability tests of four-pancake magnet are presented and discussed. The results are compared with those obtained earlier in the experiments with the smaller HTSC specimens [1–5] and are analysed by use of the scaling theory of the thermal quench [6].

2. Experimental arrangements

The magnet has been wound from Bi-2223/Ag tape (3.8 mm width × 0.24 mm thickness) with the use of

* Corresponding author. Fax: +31-53-4891099.

E-mail address: y.ilyin@tn.utwente.nl (Y.A. Ilyin).

double-pancake technology. The inner diameter of the winding is 100 mm and outer diameter is 156 mm. Total length of the HTSC tape used for the whole magnet is about 150 m. The winding is not impregnated. Instead, the tape was reinforced by 50 μm stainless steel tape. For the inter-turn insulation, the 15 μm Kapton™ tape was used. The sketch of the magnet and its photograph are shown in Figs. 1(a) and (b).

The heat drains made from 3 mm copper plates were placed between the pancakes. Their main purpose is to improve the cooling and equalise the temperature within an individual pancake as well as between the pancakes. The heat drains were connected to the cold head of the cryocooler by four copper braids – heat anchors (see Fig. 1(b)).

During the magnet fabrication, 24 potential taps (P1–24) were soldered to the tape and 20 cryogenics thermocouples Au–(0.07%Fe)–Chromel (TC1–20) were installed into the winding. The reference ends of all thermocouples were collected and connected thermally to the cold head of the cryocooler (Fig. 1(b)). Relative

positions of the potential taps and the thermocouples inside the magnet are shown in Fig. 2. The distance between neighbouring potential taps (or TCs) along the tape varies from 7.3 m for outer turns to 5.4 m for inner turns. The distance between potential taps (or TCs) in the radial direction amounts to 5 mm (see Fig. 2). Thus, we had five sections to measure voltage and five TCs per pancake. The pancakes are numbered from the top to the bottom. The lowermost pancake (#4) has a contact via 5 mm GFRP flange to the thick copper plate that was attached to the cold head of the cryocooler (see Fig. 1(b)).

Magnetic field constants calculated for inner and outer turns of four pancakes are shown in Table 1. The radial field component (perpendicular to the broad side of the HTSC tape) is about three times higher for pancakes #1 and #4. This component remains practically the same for all turns within one pancake. The axial field component (parallel to the broad side of the HTSC tape) is about three times higher for the inner turns than for outer turns within one pancake, while it changes a little

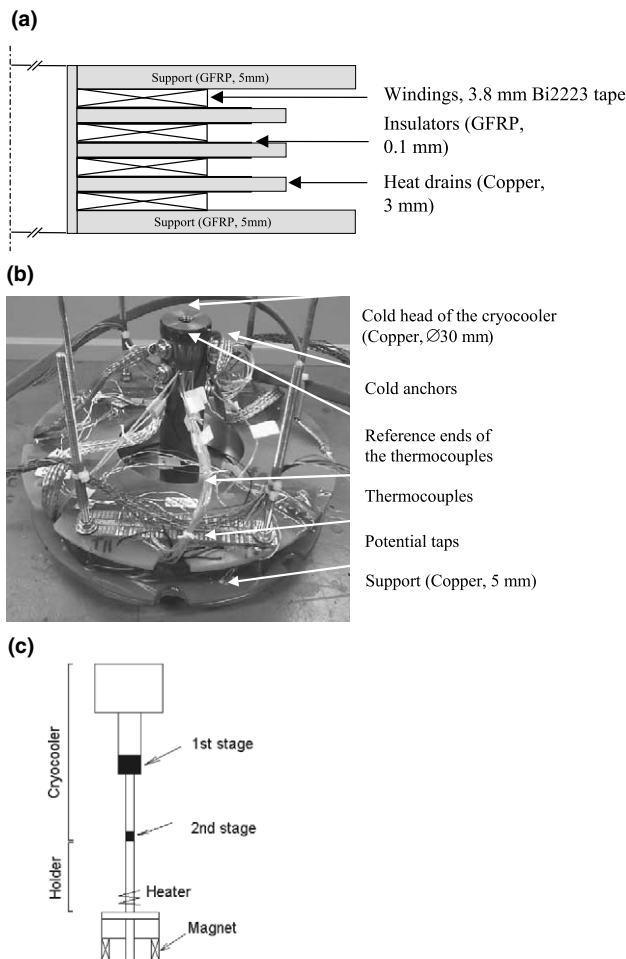


Fig. 1. (a) Sketch of the HTSC magnet (in scale), (b) the photograph of the magnet assembled for the tests, (c) general arrangement of the cryocooler and the magnet.

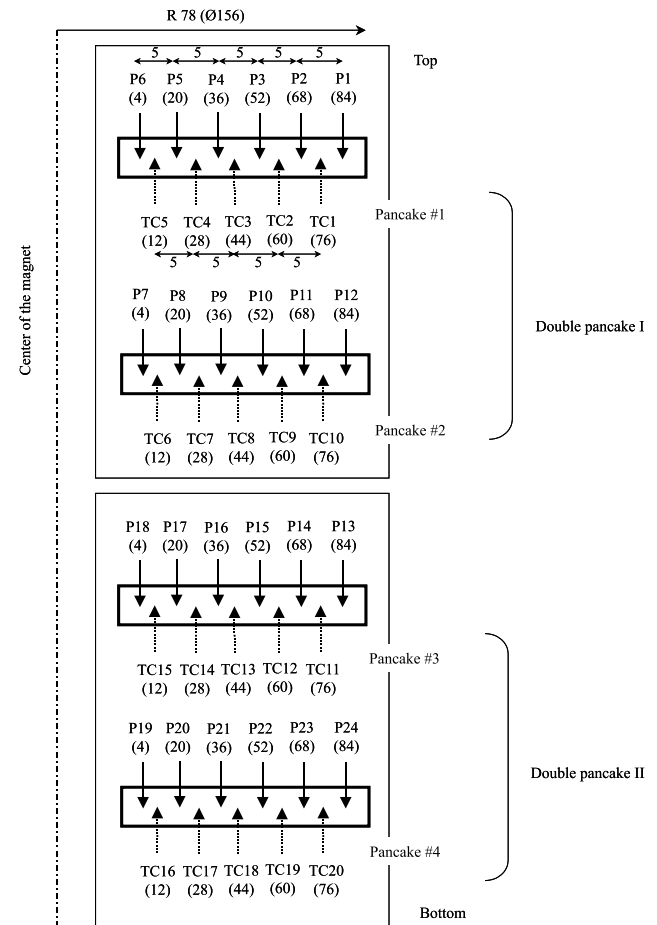


Fig. 2. Mutual positions of the potential taps (P1–24) and the thermocouples (TC1–TC20) inside the winding. The numbers of the turns corresponding are shown in brackets.

Table 1
Calculated values of magnetic field constants for inner and outer turns of four pancakes

Pancake#	Position	Bz (mT/A) (axial component)	Br (mT/A) (radial component)	B total (mT/A)
1 upper	Inner turn	5.6	2.3	6.1
1 upper	Outer turn	-1.7	2.2	2.8
2	Inner turn	6.4	0.75	6.4
2	Outer turn	-2.1	0.71	2.2
3	Inner turn	6.4	-0.75	6.4
3	Outer turn	-2.1	-0.71	2.2
4 lower	Inner turn	5.6	-2.3	6.1
4 lower	Outer turn	-1.7	-2.2	2.8

for the turns in the same radial position in different pancakes. One would expect that critical currents for pancakes #1 and #4 are lower than for pancakes #2 and #3.

First, the magnet was tested in liquid nitrogen at zero background magnetic field. Then it was mounted to the cryocooler. The sketch of the magnet mounted to the cryocooler is shown in Fig. 1(c). During all tests, the certain temperature and magnetic field were installed and the magnet was charged with the DC current at ramp rate of 2 A/s. If temperature or voltages remained stable during the measuring time, the current was increased slightly for the next run and temperature and voltage traces were recorded again. The procedure was repeated until the TQ was observed. The current between stable and unstable regimes was defined as TQC.

Two 16-channels digital analysing recorders were used to measure and store the signals from the TCs and voltage taps during the runs. These traces provided us with the data of stability and quench behaviour of the magnet. The heating power traces were obtained by multiplying of voltage and current traces. The heating power is an important characteristic in stability-quench behaviour of HTSC magnets.

3. Liquid nitrogen test

The preliminary test of the magnet has been carried out under cooling by boiling LN₂ (~77.4 K). In Fig. 3 the temperature and the heating power traces are shown for the stable regime in the magnet. In this case, the transport current in the coil is 24 A, which is about 1.6 times higher than the average critical current of the magnet determined at 1 μ V/cm (critical currents of different section are discussed in detail in Section 4). In Fig. 3 one can see that total heat release inside the magnet has been stabilised at the level of about 5 W. The highest heat release was observed in the bottom pancake #4, while the lowest one in the middle pancakes #2 and #3. The temperatures of pancakes change very little above LN₂ boiling temperature. The maximum temperature rise is ~0.05 K.

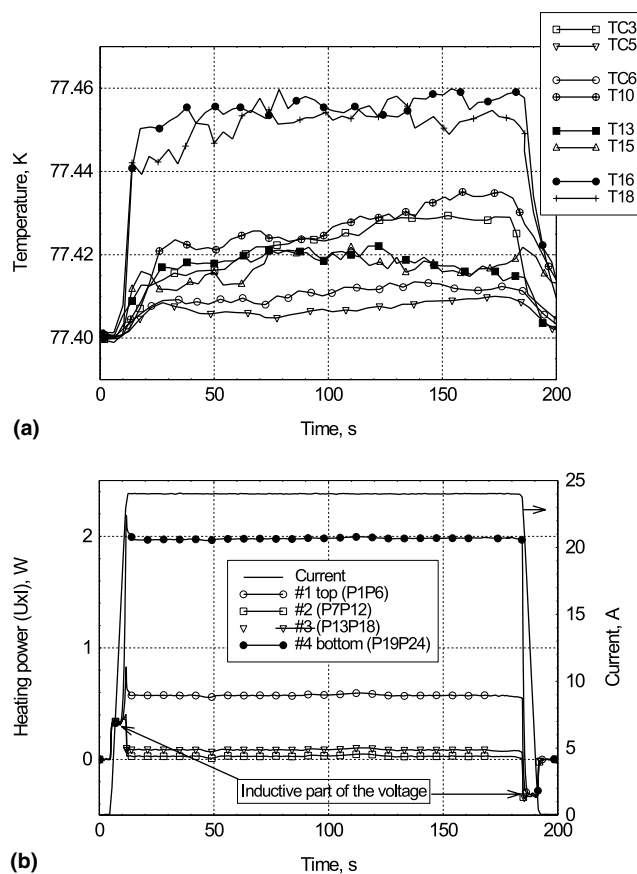


Fig. 3. Example of stable regime in the magnet at LN₂ cooling. (a) Two thermocouples in each pancake (total eight) were chosen to register the temperature change inside the magnet. (b) Internal heat release due to voltage–current characteristic is plotted for each pancake.

The small magnitude of temperature rise is not surprising, because of the extremely good cooling conditions provided by LN₂. The peak of the boiling transfer flux for LN₂ is ~15 W/cm² at 10 K temperature gradient between the surface heated and the coolant [7], though these values may vary depending on many factors. If we suppose that heat is removed through the “wet area” of the magnet, which amounts to ~450 cm² (considering no heat through the G10 flanges because of

their thickness), roughly estimated heat flux at 5 W total heat release in the magnet would be ~ 0.01 W/cm². This value is in agreement with the data of heat flux at $\Delta T = 0.05$ K in [7].

Unlike in our previous study [5], we observed a TQ in the magnet under LN₂ cooling. The transport current was 30 A, which is almost as much as twice more than magnet's average critical current. The TQ in this case is much localised. From the curves in Fig. 4 it is seen that TQ emerges in the bottom pancake #4, but only one thermocouple TC18 shows fast rise of the temperature. The other TCs show stable temperatures, a little more than the ambient one. No heating or "normal zone" propagation were detected in neighbouring sections.

The reason for the local TQ in one point is not clear. Probably it is because of a strong defect of the HTSC tape in that particular point, leading to its overheating.

The TQ development at LN₂ cooling is different from that at cryocooler cooling, when the temperature in the different parts of the entire magnet changes almost

uniformly (see Section 4). This fact can be explained by the shorter characteristic thermal length of the magnet at LN₂ cooling than at cryocooler cooling. The thermal length is a parameter that shows at what distance the temperature changes in a sample. It can be estimated as $l_T = \sqrt{kV/hS}$ [8], where k is the thermal conductivity, V is the volume of the winding, h is the heat transfer coefficient and S is the cooling surface area. The value of $h \cdot S$ can be found from the traces with the stable temperature as proposed in [6]. In our case $h \cdot S \approx 100$ W/K. Estimated values of l_T are ~ 3 cm if we assume in the formula a thermal conductivity of a silver, or ~ 0.5 cm if we assume a thermal conductivity of a stainless steel. Both lengths are much smaller than the corresponding distance between two neighbouring thermocouples along the tape and the distance between them in a radial direction.

Thus, the localisation of the heat occurs in the magnet due to very good cooling conditions. Such a localisation of the heat during a quench can be dangerous and extra attention should be paid when considering the protection of a magnet. In large coils, such non-uniform heating may cause some problems with over-voltage distributed on a short distance [9].

4. Cryocooler tests

4.1. Zero magnetic field tests

4.1.1. Critical currents and index n

After the test in liquid nitrogen, the coil was prepared for the test with cooling by a cryocooler. First, the critical currents (CC) and index n , for standard presentation of voltage current characteristics as power law, were determined in different sections of the magnet. The voltage–current (V – I) characteristics were measured at transport current with the sweep rate of 1 or 2 A/s. A $1 \mu\text{V}/\text{cm}$ criterion was used to determine CC. Fig. 5(a) shows an average CC for four pancakes as well as for the entire magnet (with error bars attributed to the CC scattering in different sections of the HTSC tape) for different temperatures of the magnet. CCs of two middle pancakes #2 and #3 are more than in top and bottom pancakes #1 and #4. The difference decreases with the temperature rise. This fact could be attributed to the self magnetic field generated inside the winding and its influence on the CC. As discussed in Section 2 and shown in Table 1, the perpendicular component of the magnetic field is less for the pancakes #2 and #3 and more for pancakes #1 and #4. That is why the highest CC was observed in the middle pancakes and the lowest in the side pancakes and particularly in pancake #4 for the whole temperature interval. At higher temperature the critical currents become smaller, thus, the influence of magnetic field is less pronounced.

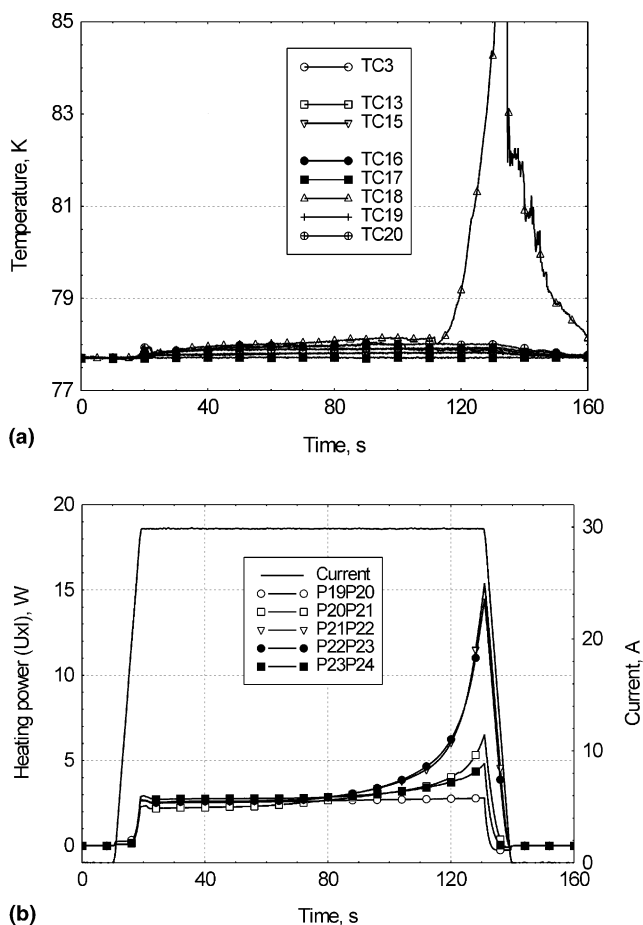


Fig. 4. Example of the thermal quench (TQ) in the magnet at LN₂ cooling. (a) Five thermocouples from the pancake #4, two from the pancake #3 and one from the pancake #2 are shown. (b) Internal heat release due to voltage–current characteristic is plotted for the section of pancake #4.

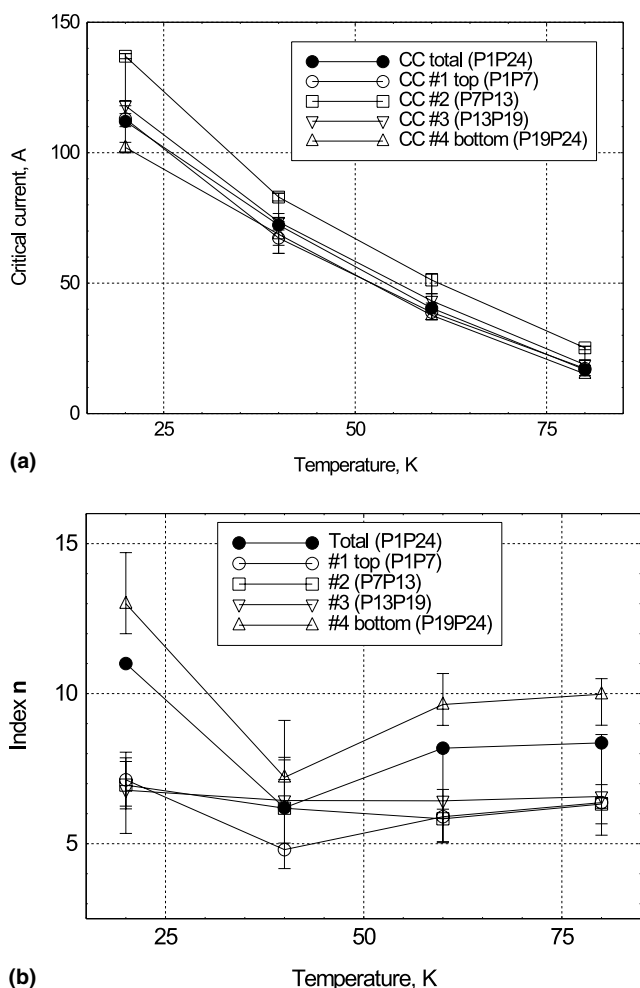


Fig. 5. (a) Critical current vs. temperature for the four pancakes and for the entire magnet. Error bars show the scattering range of the critical current in different sections of the magnet. (b) Index n for different pancakes and for the entire magnet. The error bars show the scattering of the n -values in different sections of the magnet. The connecting lines are just guidelines for eye.

Temperature dependence of the indexes n for four pancakes and the entire magnet is shown in Fig. 5(b). The error bars show the scattering of the n -values in different sections of the HTSC tape within a particular pancake. The indexes n were determined from the fitting of the V - I curves by standard expression: $E = E_0[I/I_c(T)]^n$ in the current range close to CC, where E_0 is the characteristic electric field ($E_0 = E(I_c)$) usually taken equal to $1 \mu\text{V}/\text{cm}$, I is the transport current and I_c is the critical current determined at $E = E_0$.

From Fig. 5(b) one can see that the highest n -values were observed in the bottom pancake #4 for the whole temperature interval. In middle pancakes #2 and #3 the values of index n do not change much with temperature, while in the side pancakes #1 and #4 they vary much, particularly in the pancake #4.

Several factors could cause the scattering of n -values (as well as CCs) in different sections of the HTSC tape:

inhomogeneous self magnetic field in the winding, different stress values, original scattering of the parameters in the HTSC tape along its length etc. Though it is difficult to distinguish between the rates of the contribution of all this factors, it seems to us that magnetic field dependence of the CC and index n plays the most important role in V - I curves formation for the tape inside the magnet.

The detailed analysis of index n and CC variation is not the goal of this paper. We take the experimental data on CCs and indexes n for further analysis of TQ. It is important to note the existent variation of CC and index n for the analysis and to consider how it could affect the stability and quench of the HTSC magnet.

4.1.2. Stable and unstable regime in the magnet. Thermal quench current

Like in our previous experiments [1–5], stable or quench regimes have been observed in the magnet depending on transport current level. Stable regime means saturation in temperature/voltage rise and it exists if transport current is below thermal quench current (TQC). Quench regime demonstrates very fast rise of temperature/voltage after certain time and it emerges if the transport current is higher than TQC. In Figs. 6 and 7 the stable and quench behaviour of the temperature and heating power in the magnet are shown for 20 K initial temperature and at transport current of 104 and 110 A correspondingly. One can see that despite the difference in initial values of heating power in each pancake (in #4 it is almost twice as much as in #2), the temperature rise in different pancakes is rather uniform. This is quite different from the case of LN_2 cooling where we observed strong non-uniformity. The main difference with the previous study in [5] is that characteristic time¹ of the quench process in the present magnet (~ 530 s at 20 K) is more than 10 times longer than in the small coil (~ 36 s at 20 K) with the same ratio between the transport current and TQC. This is because the volume of the magnet and, therefore, the total heat capacity are more also. In the present magnet all processes develop much slower, so there is enough time to switch off the power supply if the quench is detected.

We determined TQC of the magnet at different temperatures and magnetic fields as described in Section 2. TQC is the threshold current between the stable region (when TQ does not start, and temperature and voltages are stable nearly infinite time) and unstable region (when TQ starts after some time). In other words, TQC can be considered as a stability design criteria for HTSC coils [6,10]. In Fig. 8(a) the experimental and calculated

¹ The characteristic quench time was determined from the experimental temperature traces as an instant corresponding to minimum of the first derivative of $T(t)$ trace [6].

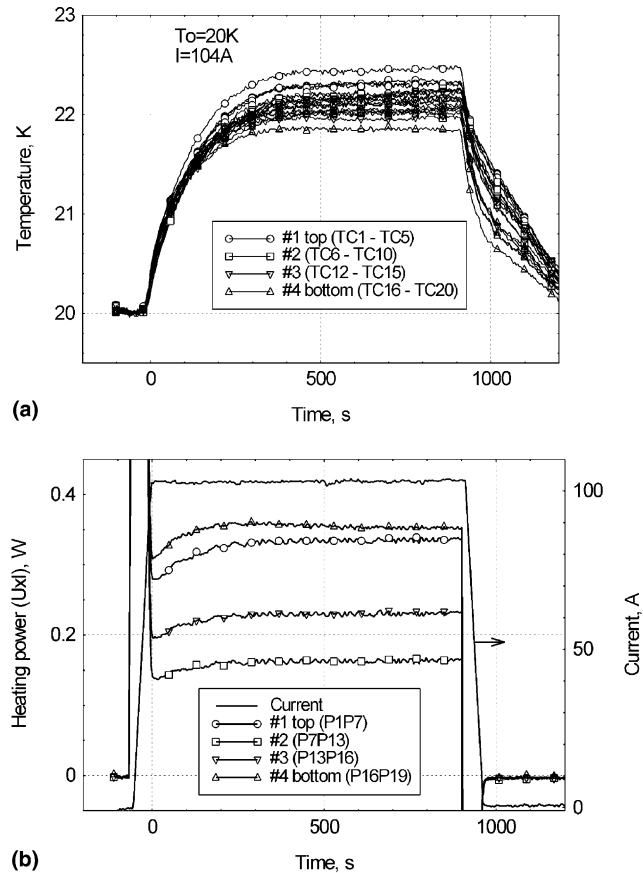


Fig. 6. Example of stable regime (temperature (a) and heating power (b)) in the magnet at cryocooler cooling at initial temperature of 20 K, 104 A transport current and zero external magnetic field. The “jumps” on the heating power curves (during ramping up and down the current) are due to inductive voltage.

values of TQC are shown. Thermal quench currents calculated by use of theory [6] are in a good agreement with the experimental data (Fig. 8(a)). One can see that for our magnet TQC is very close to the CC for the whole temperature interval and even less than CC at 20 K (TQC = 109 A and CC = 120 A). In the previous experiments with smaller specimens the TQC was ~10–15% higher than CC [1–5]. Qualitatively, it could be explained by the fact that heat is released in the volume of the device while cooling is coming from the surface, thus ‘relative’ cooling declines with the size, when the surface to volume relation reduces. In this case, relative TQC should be inversely proportional to some parameter with the dimension of the length, raised to some power [11,12].

4.1.3. Temperature non-uniformity in the magnet

Unlike our previous studies with smaller specimens, in this, relatively large magnet some sounded spatial non-uniformity in quench development has been observed. This non-uniformity depends on transport current. Temperature along the magnet was almost uniform

during the TQ if the transport current was above but very close to TQC. When the transport current becomes more, the temperature difference between pancakes is more pronounced, while within a particular pancake the temperature remains uniform. It is illustrated in Fig. 9 where the average temperature traces for each pancake are plotted for initial temperature of 60 K, and three different transport currents – 43, 46 and 48 A. TQC of the magnet at 60 K is ~39 A. Inset figures show the time dependences of the heating power in each pancake. One can see almost uniform temperature rise in all pancakes when transport current is 43 A and sufficient non-uniformity at 48 A transport current. In the later case, the temperature in the lower pancake turned into fast rise while temperatures in the other pancakes were still rising slowly. Similar temperature non-uniformities at high transport currents were observed for all initial temperatures under the cryocooler cooling.

An explanation of this phenomenon will be discussed in detail in Section 5 by using the scaling theory of thermal quench [6]. By now it would be important to note that there is an increase of the absolute heat gen-

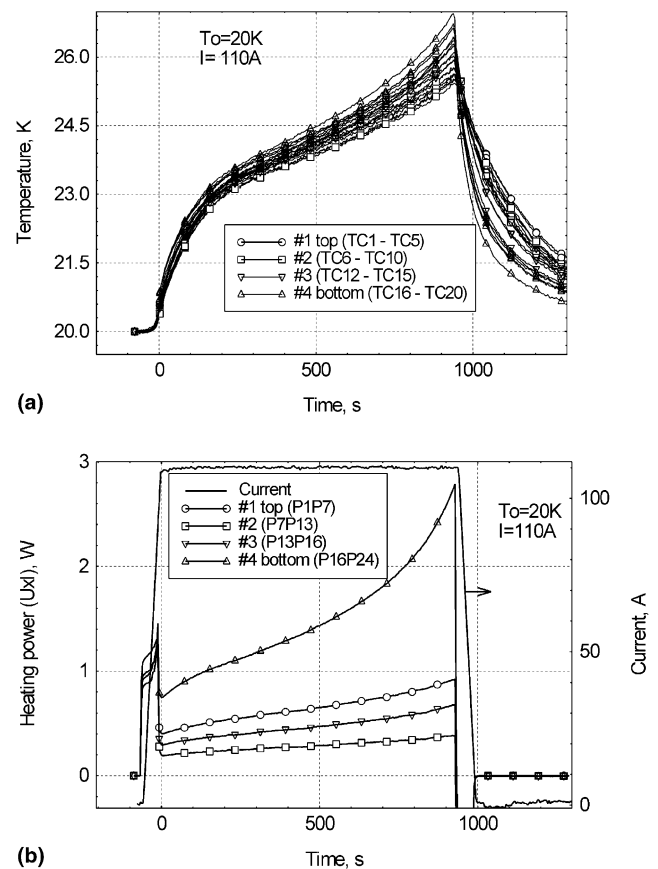


Fig. 7. Example of the thermal quench at cryocooler cooling (temperature (a) and heating power (b)) in the magnet at initial temperature of 20 K, 110 A transport current and zero external magnetic field. The “jumps” on the heating power curves (during ramping up and down the current) are due to inductive voltage.

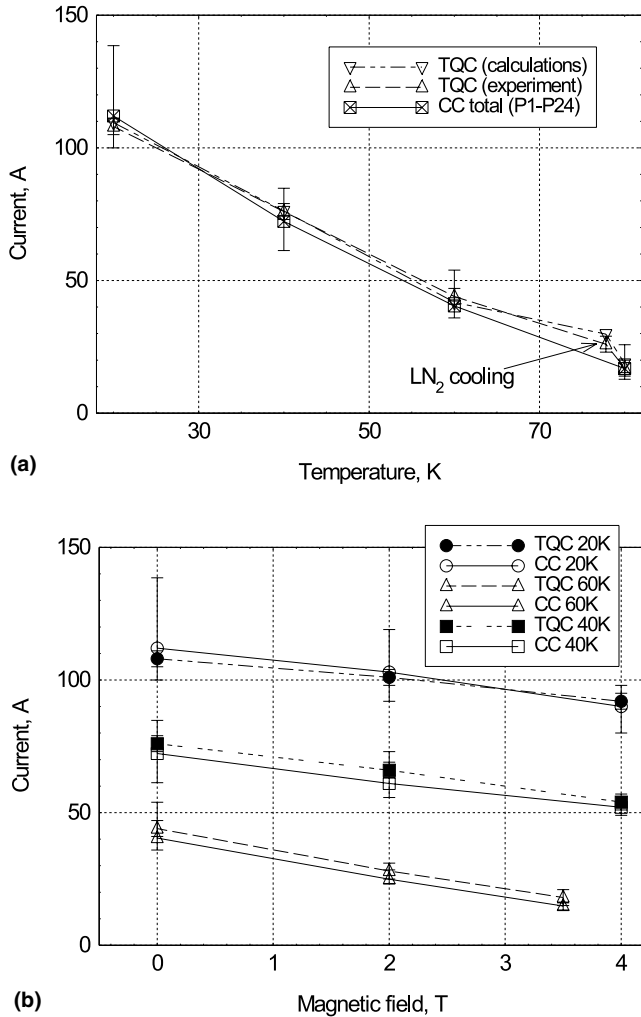


Fig. 8. (a) Measured and calculated thermal quench current and critical current vs. temperature for the entire magnet. Error bars show the scattering range of the TQC and CC in different sections of the magnet. (b) Measured TQC and CC for different values of external magnetic field. The connecting lines are just guidelines for eye.

erated in the lower pancake #4 in comparison with the other pancakes when the transport current is increased. For example, an absolute difference in initial heat generation between two side pancakes #4 and #1 at 60 K and 43 A is 0.2 W, but it is 1.25 W at 48 A. The highest heat generation in the lower pancake #4 explains the faster temperature growth in this pancake. Heating power in the lower pancake is more because the average CC for lower pancake is less than CC of the other pancakes and its *n*-value is almost twice higher than in the other pancakes (see Fig. 5).

Thus, sufficient inhomogeneity in the magnet may appear at transport currents more than TQC. In that case, an analysis of the quench parameters and estimation of the “safety” time (enough to switch off the power supply) by the theory [6] should be adjusted for non-uniform case. In principle, it could be done for the worst

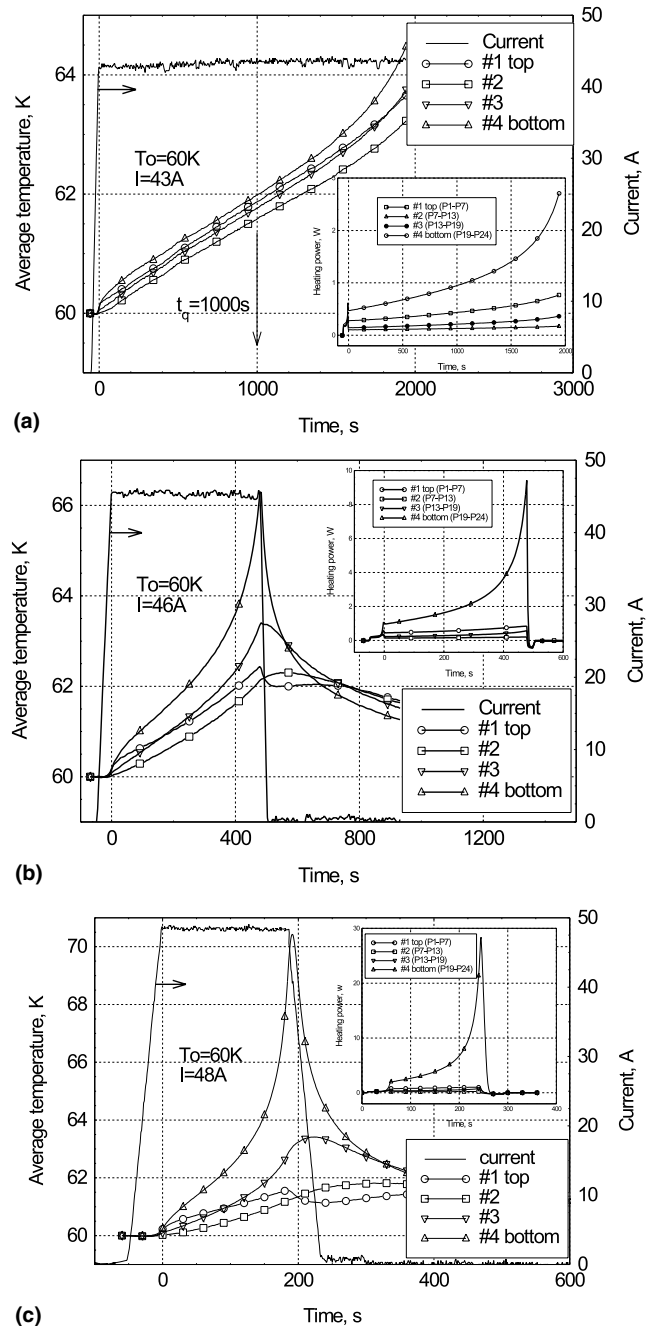


Fig. 9. Temperature non-uniformity in the magnet at 60 K initial temperature of cryocooler and three different currents (a) 43, (b) 46, and (c) 48 A. Inset pictures demonstrate evaluation of heating power in each pancake in time.

pancake(s) of the magnet where the heat generation is much more than in the other parts [6].

4.1.4. Test in external magnetic field

The magnet was also tested in external magnetic field (up to 4 T) parallel to the magnet axis i.e. to the broad side of the HTSC tape and in the same direction as the central field of the magnet. CCs of the different sections

of the magnet and TQCs were determined for 20–60 K initial temperature by the similar test sequences as we conducted at zero background field. The results are shown in Fig. 8(b).

Generally, the magnet's quench behaviour does not change. Both, stable and quench regimes were observed in the magnet depending on transport current. As can be seen from Fig. 8(b), CCs and TQCs decline with magnetic field, but the relation between them remains almost the same for all temperatures. This result is different from the results reported in [5], where the CCs decreased much more than TQCs. That was a case of a small coil with very low self-field generated. External magnetic field suppressed the CC more than 50% between 0 and 1 T. In the present case, the self-field (especially its radial component) on the tape is relatively high (see Table 1) and additional external magnetic field of the range 0–4 T does not change the CC more than 30%.

As a conclusion to experimental results, we would say that magnet's quench behaviour is generally similar to our previous results [1–5]. Nevertheless, we should mention some noticeable differences in magnet quench development as follows:

- Strong local temperature non-uniformity during the TQ at LN₂ cooling compared with good uniformity of the temperatures in each pancake under cryocooler cooling. The effect was discussed in Section 3.
- Noticeable reduction of TQ currents in relation to CC in comparison with smaller specimens.
- Much slower quench development in comparison with smaller specimens.
- Sufficient non-uniformity of temperature between pancakes during a TQ when transport current is more than TQC.

The last three items are reviewed below.

5. Discussions

5.1. Relative thermal quench current

As was mentioned in Section 4, the reduction of the relative TQC in the present magnet in comparison with the specimens measured previously is due to higher ratio between the total conductor length to cooling surface in the magnet. This ratio is an inverse effective cooling perimeter introduced in [12]. In our magnet, the total length of the conductor is 150 m. The magnet is cooled mainly through the bottom support plate and three heat drains (we do not account the cooling through the numerous potential taps and TCs as their contribution is still negligible when compared with the contribution of the heat drains). The total area of the contact between the winding and the copper plates amounts to ~ 0.011 m². Thus, the inverse effective cooling perimeter is $150 \text{ m}/0.011 \text{ m}^2 \approx 1.36 \times 10^4 \text{ m}^{-1}$. In principle, effective

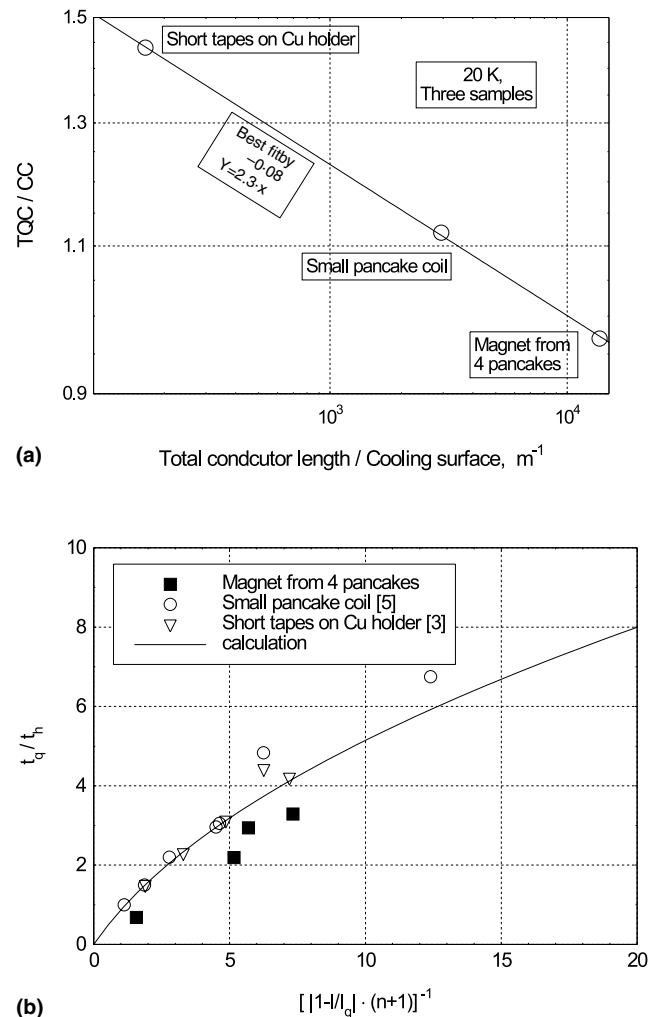


Fig. 10. (a) Relative TQC vs. the inverse integrated cooling perimeter for three different HTSC samples at 20 K. Data for short tapes and small pancake coil are from [3,5]. (b) Relative time of a quench as function of relative current and index n . Four data for the magnet correspond to cases of 20 K (108 and 110 A, $I_q = 109.2$ A) and 40 K (78 and 80 A, $I_q = 76.2$ A). Average n -values for the magnet were used.

cooling perimeter becomes less with the rise of a magnet's size.

It is illustrated in Fig. 10(a), that for small specimens with relatively high cooling perimeter, the relative TQC is higher than for the present magnet. Similar results were discussed in [11] for different HTSC magnets described in the literature. The experimental data in Fig. 10 are fitted by the power law with the degree of $(-1/(n+1))$ [11]. The derived n -value of 11.5 is close to average n -value for the magnet in most experiments at 20 K. These results support the theory and previous conclusions done in [6] that for better evaluation of quench parameters of large specimens, the results from the small model could be used. For example, the data obtained from the test of small single pancake coil [5]

may be used to evaluate TQC of four-pancake magnet with good accuracy.

5.2. Thermal quench characteristic time

Despite the fact that quench process in the magnet goes much slowly compared with that of small specimens, the ratio between the characteristic time of a quench t_q [6] and characteristic thermal time t_h [6] remains the same for the same transport current to TQC ratio:

$$\frac{t_q}{t_h} = \sqrt{\frac{2I_q}{|I - I_q|(n+1)}} \tan^{-1} \left(0.5 \sqrt{\frac{2I_q}{|I - I_q|(n+1)}} \right). \quad (1)$$

Here I is the transport current and I_q is the TQC. The characteristic thermal time is given by $t_h = CV/hS$ [6], where V is the volume of the coil, C is the specific heat, S is the cooling area, and h is the heat removal coefficient. The product of $h \cdot A$ can be derived from the saturated heating power traces in stable regime as it was proposed in [2,6]. For example, this product is equal to ~ 0.83 W/K for 40 K and 78 A in the magnet. The product of $C \cdot V$ for the magnet can be calculated using well-known formula for composite materials [6]: $C \cdot V = \sum_i C_i \cdot V_i$, where V_i and C_i are volume and volumetric heat capacity of each material component correspondingly. For the present magnet the value of $C \cdot V$ was estimated to be equal to ~ 297 J/K at 40 K, and finally $t_h = 357.8$ s and $t_q/t_h = 3.4$. The data for heat capacities are taken from [7].

The relative quench time (t_q/t_h) for different specimens is plotted in the Fig. 10(b) as a function of transport current, TQC and index n . The results from three different specimens are in a good agreement with the theory [6]. Thus, the theory and the results from small models could be used to predict the characteristic quench time for larger coils. The slower quench development is determined by the higher effective heat capacity due to larger total mass of the magnet.

5.3. Pancake-to-Pancake temperature inhomogeneity

As far as quench develops in a HTSC device uniformly, i.e. the temperature rise is almost equal in all parts of a device, it can be considered as continuum with its parameters averaged and the theory [6] can be applied directly. However, in a real device some non-uniformity exists as shown in Fig. 9. The question is how to apply the theory for such non-uniform case.

As discussed in Section 3, strong temperature non-uniformity may occur if the characteristic thermal length of an object is smaller compared with actual object size. In a case of strong cooling (LN₂), the thermal length of the magnet was estimated to be of order of several

centimetres. On the contrary, under the cryocooler cooling, the estimated thermal length for each pancake of our magnet is ~ 1.43 m at 20 K and ~ 0.61 m at 60 K if we consider the heat conductivity along the HTSC tape, and ~ 0.52 m at 20 K and ~ 0.27 m at 60 K if we consider the heat conductivity across the HTSC tape. Indeed, these values are higher than the dimensions of a pancake and even the magnet. For the estimation of thermal length we used the same formula as in Section 3 together with the data about heat conductivity in HTSC windings from [13]. The data about effective cooling were taken from the experiments with the stable regimes, and they are 0.81 W/K at 20 K and 0.65 W/K at 60 K.

Thus, one can expect that temperature within each pancake and even within the magnet should be uniform even with non-uniform heat release in the magnet. Yet, this is true for static case or very slow quench development. The example is shown in Fig. 9(a) for $I = 43$ A, where the temperature in four pancakes is almost uniform despite the stronger heat release in bottom pancake #4. It is seen that characteristic time of the process (t_q) is about 1000 s that is comparable with the estimated thermal time (t_h) of 1000–2000 s for our magnet. However, when transport current increases (Fig. 9(b) ($I = 46$ A) and Fig. 9(c) ($I = 48$ A)) and difference between transport current and TQC becomes more, the t_q decreases and becomes substantially smaller than t_h . Besides that, t_q is different for different pancakes due to difference in t_h (because of slight difference in cooling) and n -values (see expression (1)). There is not enough time for the temperature to equalise among pancakes. Therefore, each pancake behaves “independently” and bottom pancake #4 (with higher heat release) quenches earlier.

Thus, for uniform temperature distribution within the magnet, the time of quench process t_q (mostly determined by the difference between transport current and TQC [6]) should be comparable or higher than the characteristic thermal time t_h : $t_q \geq t_h$. If the quench time t_q is less than characteristic thermal time t_h , the temperature non-uniformity may appear. For such case, the theory [6] can be applied for each pancake because the temperature within each pancake stays uniform.

6. Summary

Quench development in the heavily instrumented, four-pancake magnet, has been investigated at different ambient temperatures and background magnetic fields. Generally, the quench development of the magnet is similar to that observed earlier in smaller specimens and can be analysed by use of the universal scaling theory for quench in HTSC devices [6]. Stable and unstable regimes do exist in the magnet when transport current is less or higher than the thermal quench current. Thermal

quench current has been determined for different cooling conditions and different temperatures. It declines with temperature and can be calculated with good accuracy by use of the theory of thermal quench [6]. Dependence of relative thermal quench current on external magnetic field is less pronounced due to high self-field of the magnet.

Thermal quench current of the magnet was found to be close or even less than critical current determined by the $1 \mu\text{V}/\text{cm}$ criterion. This can be explained by smaller value of the effective cooling perimeter of the magnet in comparison with the previously tested specimens.

Quench develops in this magnet relatively slowly compared with the smaller specimens. Increase of characteristic thermal time can be attributed to larger mass of the magnet and, therefore, higher value of its effective specific heat.

At LN_2 noticeable temperature non-uniformity and heat localisation were observed during the quench. The effect can be explained by the shorter thermal length of the magnet at LN_2 cooling.

Some non-uniformity of the temperature among different pancakes has been observed under cryocooler cooling if transport current is sufficiently higher than the thermal quench current, while within each pancake temperature remained almost uniform. This is because at higher currents, the characteristic time of the quench process is smaller than characteristic thermal time and there is not enough time for temperature to equalise. In a case of temperature non-uniformity, the theory [6] should be applied separately for each pancake.

It was confirmed, that using theory [6] and results from the small models it is possible to predict the quench parameters of larger coils.

Acknowledgements

Authors would like to express their gratitude to Sumitomo Electric Industries Ltd. for manufacturing of the experimental coil. Authors are very grateful to their

students K. Ohya, D. Utsunomiya and S. Noda for their great help in experiments and data proceedings.

References

- [1] Vysotsky VS, Takeo M, Kiss T, Ilyin YuA, Matsuo M, Nakamura T, et al. The stability characteristics of Bi-based high temperature superconducting coil. In: Proceedings of the MT-15 Conference. Beijing, China: Science Press; 1998. p. 1056–9.
- [2] Kiss T, Vysotsky V, Yuge H, Saho H, Ilyin Yu, Takeo M, et al. Heat propagation and stability in a small high T_c superconductor coil. *Physica C* 1998;310:372–6.
- [3] Vysotsky VS, Kiss T, Ilyin Yu, Takeo M, Saho H, Funaki K, et al. Heat and quench propagation in HTSC coils with bobbins from different materials. Part 1: Experiment. In: Proceedings of the ICEC-17 Conference. Bristol and Philadelphia, UK: Institute of Physics Publishing; 1998. p. 583–6.
- [4] Vysotsky VS, Kiss T, Ilyin Yu, Takeo M, Saho H, Funaki K, et al. Heat and quench propagation in HTSC coils with bobbins from different. Part 2: Results and their discussion. In: Proceedings of the ICEC-17 Conference. Bristol and Philadelphia, UK: Institute of Physics Publishing; 1998. p. 357–60.
- [5] Vysotsky VS, Ilyin YuA, Kiss T, Inoue M, Takeo M, Irie F, et al. Thermal quench study in a HTSC pancake coil. *Cryogenics* 2001;40(1):9–17.
- [6] Rakhmanov AL, Vysotsky VS, Ilyin YuA, Takeo M. Universal scaling law for quench in HTSC devices. *Cryogenics* 2000;40(1):19–27.
- [7] Iwasa Y. Case studies in superconducting magnets. New York: Plenum Press; 1994.
- [8] Gurevich AV, Mints RG, Rakhmanov AL. The physics of composite superconductors. New York: Beggel House; 1997.
- [9] Paasi J, Lehtonen J, Kalliohaka T, Mikkonen R. Stability and quench of a HTS magnet with a hot spot. *Supercond Sci Technol* 2000;13:949–54.
- [10] Ishiyama A, Asai H. A stability criterion for cryocooler cooled HTS coils. *IEEE Trans Appl Supercond* 2001;11(1):1832–5 (Part 2).
- [11] Vysotsky VS, Ilyin YuA, Rakhmanov AL, Takeo M. Quench development analysis in HTSC coils by use of the universal scaling theory. *IEEE Trans Appl Supercond* 2001;11(1):1824–7 (Part 2).
- [12] Vysotsky VS, Ilyin YuA, Kiss T, Ohya K, Utsunomiya D, Noda S, et al. Stability and quench study of the Bi-2223 based HTSC coil. In: Proceedings of the ICEC18. Mumbai: Narosa Publishing House; 2000. p. 243–6.
- [13] Lehtonen J, Mikkonen R, Paasi J. Effective thermal conductivity in HTSC coils. *Cryogenics* 2000;40:245–9.